Available online at www.sciencedirect.com

ScienceDirect

journal homepage: www.elsevier.com/locate/issn/15375110

Research Paper

Using slurry pit headspace gas concentrations to quantify pit ventilation rate in a dairy house. Comparison between a closed and slatted floor

Carsten C.A. Schep [a,*], Hendrik Jan H.J.C. van Dooren [a], Peter P.W.G. Groot Koerkamp [b], Nico N.W.M. Ogink [a]

[a] Wageningen UR Livestock Research, P.O. Box 338, 6700 AH Wageningen, the Netherlands
[b] Farm Technology Group, Wageningen University, P.O. Box 16, 6700 AA, Wageningen, the Netherlands

ARTICLE INFO

Article history:
Received 18 May 2022
Received in revised form
8 September 2022
Accepted 9 September 2022
Published online 27 September 2022

Keywords:
Dairy
slurry
pit
floor types
ammonia
emission

Ammonia mitigation systems in dairy houses with a slurry pit below, often close off the pit to limit air circulation between the pit and the house. Currently, the effect of limiting air recirculation on emission is unknown. Experiments were carried out to understand the effect of closing off the pit on NH_3 emissions. This study aimed to (1) develop a method to quantify continuous pit air flow rate, (2) provide information about gas concentrations inside a slurry pit and (3) determine the effect of closing off the floor on air exchange rate between pit and house. Mass balances for CO_2 and CH_4 were set up to quantify air exchange rate between pit and house based on natural slurry production. The applicability of this approach was tested for both a conventional slatted floor as well as for an NH_3 mitigating closed floor. The ventilation rate estimates of the mass balance were compared to the ventilation rate as determined with a rate-of-decay (ROD) experiment. Quantification of pit ventilation rate based on the CO_2 and CH_4 mass balances is most appropriate to discover relative differences. Pit ventilation rate turned out to be temperature dependent and therefore showes a clear day–night pattern with ventilation rates during the night. The ROD method provided a more accurate quantification of the ventilation rate and showed replacement rates during daytime of 4.3–7.3 h^{-1}.

1. Introduction

The dairy sector is facing huge challenges in reducing ammonia (NH_3) and methane (CH_4) emissions. Ammonia depositions lead to eutrophication and acidification of the soil, resulting in loss of biodiversity (Heij & Schneider, 1991). Methane enhances the greenhouse effect (Knapp, Laur, Vadas, Weiss, & Tricarico, 2014), resulting in global temperature rise which increases the likelihood for extreme weather events (Solomon et al., 2007) and an increased risk of human or animal diseases (Moss, Jouany, & Newbold, 2000). Apart from environmental impact, both ammonia and methane emissions reduce overall agricultural system efficiency since they

* Corresponding author. Postbus 338, 6700 AH Wageningen, the Netherlands.
E-mail address: carsten.schep@wur.nl (C.A.(C.) Schep).
https://doi.org/10.1016/j.biosystemseng.2022.09.002

Nomenclature

A_{fc}	Covered slurry area of the flux chamber corrected for 0.01 m sinking into the slurry (m^2)
A_i	Slurry area of alley i
a_x	Slope of the gas concentration in the flux chamber over time ($g\ m^{-3}{}_{fc}\ s^{-1}$)
$C_{x,i}$	Gas concentration of gas x in alley i ($g\ m^{-3}$)
$C_{x,i}[ppm]$	Gas concentration of gas x in alley i (ppm)
$C_{x,i,j}[ppm]$	Average gas concentration of gas x in alley i at day j (ppm)
$C_{x,i,hs}$	Mean headspace concentration of gas x in alley i ($g\ m^{-3}$)
$C_{x,in}$	Concentration of inflowing air of gas x ($g\ m^{-3}$)
$C_{x,i,out}$	Concentration of outflowing air of gas x from alley i ($g\ m^{-3}$)
$C_{x,i,0,hs}$	headspace concentration at $t = 0$
$CV_{x,i}$	Coefficient of variation of the concentration of gas x in alley i (–)
$CV_{x,i,j}$	Coefficient of variation of the concentration of gas x in alley i within day j (–)
Fc	Flux chamber for gas production rate measurements
IQR	Interquartile range
M_{air}	Molar mass of air (28.96 $g\ mol^{-1}$)
M_x	Molar mass of gas x (CO_2: 44.01 $g\ mol^{-1}$ or CH_4: 16.04 $g\ mol^{-1}$)
PR_x	Slurry production rate of gas x ($g\ m^{-3}\ h^{-1}$)
Q_1	First quartile
Q_3	Third quartile
ROD	rate-of-decay
$SD_{x,i}[ppm]$	Standard deviation of the concentration of gas x in alley i ($g\ m^{-3}$)
$SD_{x,i,j}[ppm]$	Standard deviation of the concentration of gas x in alley i within day j ($g\ m^{-3}$)
SL	Slurry level (m)
TAN	Total ammoniacal nitrogen
V_{fc}	Volume of the flux chamber ($m^3{}_{fc}$)
$V_{hs,i}$	headspace air volume in alley i (m^3)
$V_{sl,i}$	Slurry volume in alley i (m^3)
VR_i	Ventilation rate through alley i ($m^3\ h^{-1}$)
WR_x	Slurry withdrawal rate of gas x ($g\ h^{-1}$)
β_1,β_2	Regression coefficients
ρ_{air}	Density of air at 12.7 °C ($1.22 \cdot 10^3\ g\ m^{-3}$)

are a leakage in the nitrogen and carbon cycles (Sutton, Erisman, & Oenema, 2007). To reduce the impact on the environment and increase efficiency, emission limits and objectives have been set for both ammonia and methane (EEA, 2016; European Commission, 2020).

Methane emission has a negative impact on a global scale whereas the impact of ammonia is more regional and causes problems in areas with high livestock densities such as the Netherlands. In the Netherlands, dairy farming is responsible for 56% of national ammonia emission (Bleeker, Sluis, & Schijndel, 2018; Hoogerbrugge et al., 2019). On a global scale, agriculture is responsible for 40% of methane emissions from anthropogenic sources (CCAC, 2017). The dairy livestock sector contibutes 4.0% to the total global greenhouse gas emission expressed in CO_2-equivalents (Gerber, Vellinga, Opio, Henderson, & Steinfeld, 2010), but is increasing as a result of an increasing milk production worldwide. Therefore, the relative contribution of the dairy sector is expected to increase towards 2050 (FAO & GDP, 2018).

Emission processes involving ammonia and methane differ. Ammonia is produced from urea, which is the main nitrogenous component of dairy urine and is catalysed by the enzyme urease (Aguirre-Villegas et al., 2017). Since urease is abundantly present in cow faeces, conversion of urea to ammonia is inevitable. Ammonia compounds are converted to ammonium until a pH-dependent equilibrium is reached. Ammonia release to the air is dependent on a chemical equilibrium between liquid ammonia in the urine puddle and gaseous ammonia in the air. Ammonia volatilises from the floor and slurry surface (Snoek, Stigter, Ogink, & Groot Koerkamp, 2014). Methane is the product of an anaerobic degradation process of organic matter in which a complex microbial community is involved. This process occurs in the cows rumen and in manure storages (Hindrichsen, Wettstein, Machmüller, & Kreuzer, 2006). Several pathways for methane formation are present either consuming or producing carbon dioxide (Buswell & Mueller, 1952). The rate of CH_4 production from manure can be influenced by changing the bacterial pool size or bacterial activity (Van Dooren et al., 2007).

Dairy housings in the Netherlands typically include slatted floors with a slurry pit below. Here, the contribution of the slurry pit to total house emission is 30–50% for NH_3 (Mosquera et al., 2017; Ogink, Groenestein, & Mosquera, 2014) and 16–30% for CH_4 (Huis in 't Veld & Monteny, 2003; Šebek & Schils, 2006). Different techniques are present to reduce emissions of ammonia and CH_4 from the slurry pit. Ammonia emission from the slurry pit is currently mitigated by closing off the floor to reduce air flow rate through the slurry pit such that less ammonia volatilises as a result of increased concentrations. Methane emissions can be reduced by suppressing the microbial activity through (1) aeration of slurry, (2) cooling of slurry or (3) frequent removal of slurry (Amon, Kryvoruchko, Amon, & Zechmeister-Boltenstern, 2006; Chadwick et al., 2011; Hindrichsen et al., 2006; Starmans, Blanken, Kupers, & Timmerman, 2009).

In the Netherlands, approved ammonia emission mitigation methods are listed in the Rav-list (TacRav, 2018). Prior to listing, provisional emission factors of prototypes of new floor systems are predicted using the Snelstal model (Monteny, Schulte, Elzing, & Lamaker, 1998) and measured at different farms according to a measurement protocol to establish emission factors (Ogink, Mosquera, & Hol, 2017). Most low-emission floor systems are based on a quick removal of urine puddles together with limited air circulation between the slurry pit and house. Yet modelling the effect of limiting air recirculation on emission is a challenging task. Direct measurement of pit emissions would require information on the air flowrate through the slots of the slatted floor which is complex due to temporal and spatial variations between slots. The Snelstal model does not use the air flowrate through the slats but determines the emission from the slurry pit under a slatted floor by estimating the surface, pH and total ammoniacal nitrogen (TAN) content of the slurry top layer, and the air flowrate over the slurry surface. The model assumes that air velocity at slurry surface level is 33% of air velocity at floor level. Effect of restricting air exchange by semi-closed floors are expressed as an assumed 90% reduction of the pit emission in case of a slatted floor. Monteny et al. (1998) suggested improved modelling of air exchange dynamics between slurry pit and house air. To date, several studies have investigated airflow behaviour in the slurry pit. Qin et al. (2020) found significant effects of the slatted floor layout and air velocity on the air exchange rate between the slurry pit and house using a computational fluid dynamics modelling approach. Ye et al. (2009) concluded based on a scale model of a slurry pit that ventilation rate, air exchange area and slurry level affect the air flow pattern in the slurry pit as well as the air exchange rate. Based on measurements in practise, Monteny, Bot, Raaben, and Overbeek (2000) found a linear increase in the flow rate when the outside air temperature dropped below house temperature. This effect is probably due to thermal buoyancy, that is the cold inlet air replaces the warm pit air because of density differences.

To gain knowledge about air flow rate in the slurry pit and the effect of closing off the pit on ammonia, an experimental study was carried out. The objectives of this study were to (1) develop a method for continuous pit air flow rate quantification, (2) provide information about gas concentrations inside a slurry pit and (3) determine the effect of closing off the floor on air exchange rate between pit and house.

2. Materials and methods

Three independent methods to quantify pit ventilation rate were compared in this study to quantify the effect of a closed floor compared to a slatted floor. Two methods were based on the pit headspace mass balances of CO_2 and CH_4 for which input, output and manure production were measured. The third method was based on a rate-of-decay (ROD) experiment with CO_2 as tracer gas. Measurements were taken in two identical emission measurement units (unit A and B) at the Dairy Campus, the experimental dairy farm of Wageningen Livestock Research in Leeuwarden between March 13th 2019 and April 18th 2019. Unit A was equipped with a standard slatted floor and unit B with a closed floor and a manure scraper. Every four or five days, measurements switched between unit A and unit B as shown in Fig. 1. The ROD experiment was carried out on May 28th 2019 in unit A.

2.1. Dairy house characteristics

A schematic representation of the measurement units is given in Fig. 2. Units A and B were located next to each other in one building and separated by a wall and a door on the feeding alley to minimise air exchange. The units had a capacity of 16 cows each and an occupancy 100% during the measurement period. Each unit was mechanically ventilated with two Fancom 1680 M fans with a maximum capacity of 20,750 $m^3\ h^{-1}$. The fans were set at a ventilation capacity of 50%. The side walls were closed with a curtain to reduce the effect of wind on ventilation rate. Cows were milked twice a day in another building around 06:00 and 16:00. On these moments no cows were present in the building for about 2 h per milking event.

Both units had a separate slurry pit with a depth of 1.3 m and a volume of 177 m^3. The pit was divided in 5 alleys (Fig. 2A). Slurry was levelled out between alleys via gaps with a diameter of 0.5 m at the bottom of the pit walls. A slurry level of 0.35 m was present at the start of the experiment. At a slurry level above 0.5 m, air exchange was possible only between alley 2 and 3 and between alley 4 and 5.

The alleys differed in width resulting in slurry surface areas of 34.9 m^2, 24.0 m^2, 24.0 m^2, 24.0 m^2, 29.6 m^2 for alley 1 to 5 respectively.

2.2. Measurement equipment

Unit A was equipped with a conventional slatted floor and unit B with a grooved closed floor ('V1 Groove vloer', V17 Agro, Oosterbeek, NL). The closed floor was scraped once per hour and slurry was deposited to the pit beneath the unit via the slurry disposals as shown in Fig. 2B. Inside the slurry pit of both unit A and B, 12 sampling points were installed at the bottom side of the floor. 16 mm polyethylene (PE) tubes were installed as protection for the 6 mm PE sampling tubes. The sampling tubes were able to move within the protection tubes such that the sampling height could be adjusted. House air composition was measured via a sampling point in the middle of the unit at a height of 4.5 m. The sampling points were connected to a 12-channelled manifold. Instead of sampling point 4 (Fig. 2B), sampling point 0 (Fig. 2A) was connected. The sampling points were measured sequentially with a FTIR measurement device (Fourier-Transform InfraRed spectroscopy; Gasmet technologies, Vantaa, Finland; accuracy: ±1%).

2.3. Mass balance

The five pit alleys were considered as individual experimental units. Therefore, a mass balance of the headspace for each alley i was set up with Eq. (1).

$$V_{hs,i}\frac{dC_{x,i,hs}}{dt} = VR_{hs,i}*C_{x,in} - VR_i*C_{x,i,out} + PR_x*V_{sl,i} - WR_x*V_{sl,i}\left(g\ h^{-1}\right) \tag{1}$$

Here, $V_{hs,i}$ represents headspace air volume in m^3 for alley i; $C_{x,i,hs}$, $C_{x,in}$, and $C_{x,i,out}$ concentrations ($g\ m^{-3}$) of gas x (CO_2 or

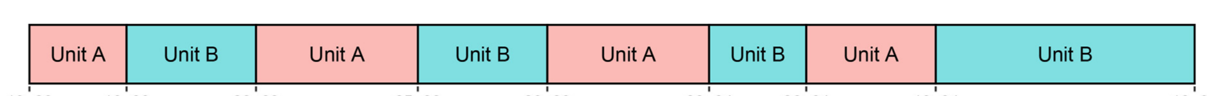

Fig. 1 – Schematic representation of the measurement periods per unit (A or B) from March 13th 2019 up to April 18th 2019. On the dates presented at the x-axis, additional measurements were carried out.

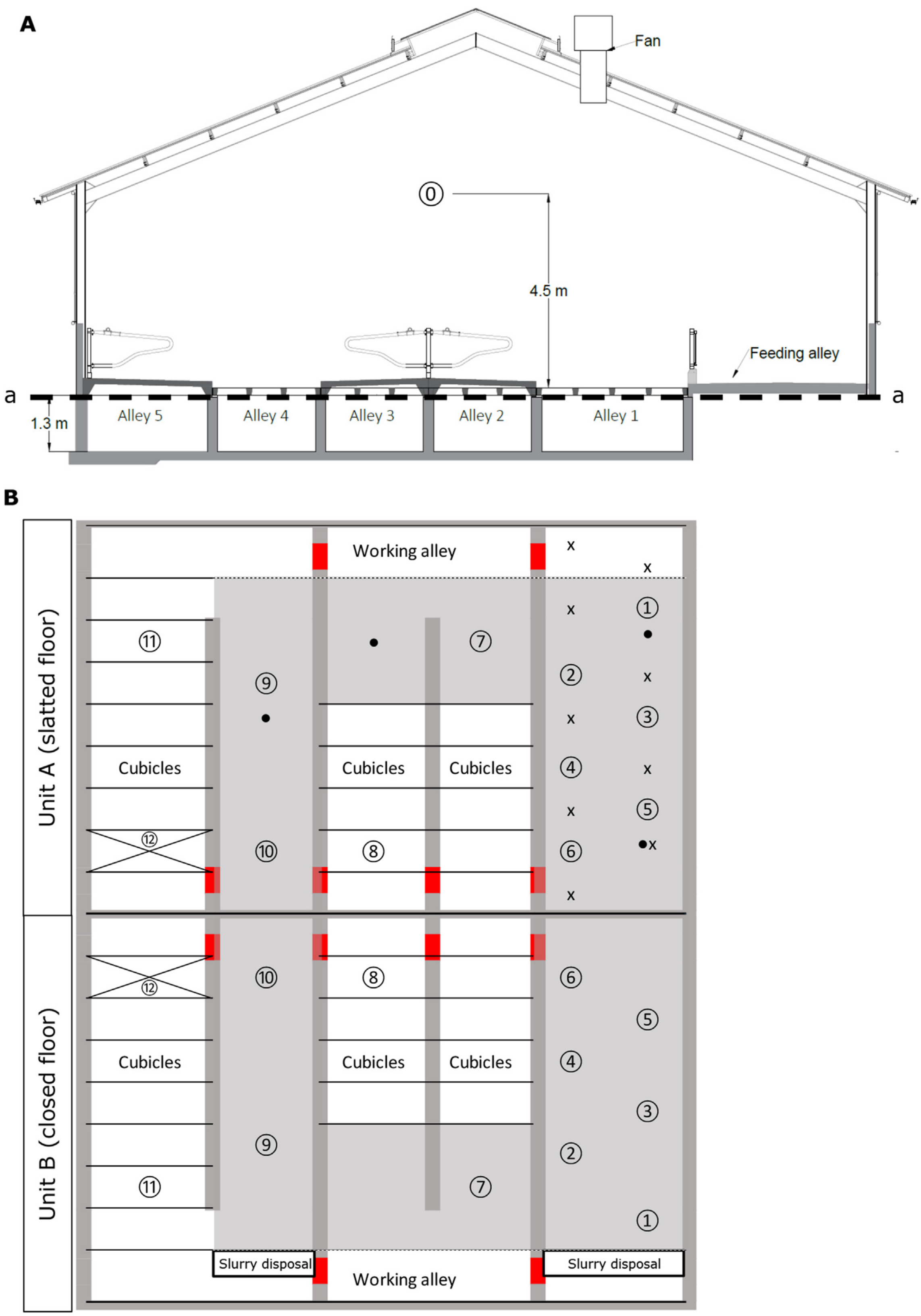

Fig. 2 — The cross-section of a measurement unit in A and a top view from the a–a line of the headspace area in B. B shows the pit walls beneath the house. Light grey areas represent a slatted or closed floor. Gaps at the bottom of the slurry pit to level out the slurry are indicated in red and have a diameter of 0.4 m. Sampling point locations are indicated with numbers ⓪ to ⑫. Sampling points were mounted at the bottom of the slatted floor and adjustable in height. Measurement locations for gas production rate were indicated with: ●. Injection points for the ROD experiment were marked with an 'x'. (For interpretation of the references to color in this figure legend, the reader is referred to the Web version of this article.)

CH_4) in respectively headspace, inflowing and outflowing air. The time interval *dt* between two measurements was 2 h. VR_i is the ventilation rate through headspace *i* in $m^3\ h^{-1}$. PR_x and WR_x are production and withdrawal rates of gas x in $g\ m^{-3}\ h^{-1}$ by the slurry. In this study, headspace air and house air were assumed to be two separate ideally mixed volumes. Withdrawal was assumed to be zero.

House air was assumed to be perfectly mixed due to the high ventilation rate (16 replacements per hour) and represented air flowing into the headspace. House air was measured at point 0 (Fig. 2A).

2.4. Concentration of outflowing air

Average headspace air concentrations per alley were assumed to represent air flowing out of the pit. The headspace was defined as the volume of air between slurry and the bottom of the floor. To determine the sampling height in the headspace, sampling points were set at different heights: (1) 0.1 m above slurry level, (2) halfway the headspace and (3) 0.1 m below the floor. Since no significant differences were found, sampling points were placed halfway the headspace. Every four or five days, sampling height was adjusted according to the increased slurry level.

Each sampling point was measured for 10 min of which the last 5 min were used for further analysis. The first 5 min were needed for a full refreshment of the measurement chamber. The channels which were not measured, were continuously refreshed at a flow rate of $0.25\ l\ min^{-1}$.

2.5. Gas production rate

Production rates of CO_2 and CH_4 by the slurry were measured on the days that continuous measurements switched between the units (Fig. 1). Additional gas production rate measurements were taken at April 15th. Gas production rates were determined by measuring the accumulation of CO_2 and CH_4 in a static flux chamber (Ogink, Mosquera, Calvet, & Zhang, 2013). The flux chamber was pyramid shaped with a size of 1.04 × 0.46 × 0.23 m (L × W × H) and was foldable such that it could enter the pit through the slots of the slatted floor. Since unit B was equipped with a closed floor, gas production rates were only measured in unit A and assumed to be similar for unit B.

During a measurement, an air sample was taken with the flux chamber at 0.1 m above slurry level. Thereafter, the flux chamber was put on the slurry. It took 3 min to get one datapoint existing of 2 min flushing and a 20 s analysis for each of the gases CO_2, CH_4 and NH_3. Air drawn from the box was recirculated to the flux chamber. After correcting the datapoints for calibration, production rates a_x were determined by a linear regression through the measurement points. Next, the production rate PR_x of gas *x* by the slurry was calculated with Eq. (2):

$$PR_x = \frac{V_{fc} * a_x}{A_{fc} * SL} * 3600 \left(g\ m^{-3}_{slurry} h^{-1}\right) \tag{2}$$

where *x* represents CO_2 or CH_4. V_{fc} and A_{fc} are volume (m^3) and covered slurry area (m^2) of the flux chamber (fc), corrected for 0.01 m sinking into the slurry. a_x is the slope of the concentration increase in the flux chamber obtained by linear regression ($g\ m^{-3}{}_{fc}\ s^{-1}$) and *SL* the slurry level (m).

To exclude potential spatial variation in gas production rate throughout the slurry pit, four measurements were averaged such that a single value per day was used for calculation in the mass balance. The four measurements were divided throughout unit A as shown in Fig. 2B. Production rate measurements were executed every four or five days. Between measurements, production rate values were interpolated.

Production rates could not be determined for unit B since the flux chamber could not enter the slurry pit with a closed floor. Therefore, CO_2 and CH_4 production rates in unit B were assumed to be equal to those measured in unit A.

2.6. Measurement devices

The FTIR for measuring the gas concentrations of CO_2, CH_4 and NH_3 in the pits had a continuous throughput of sample air and triggered the manifold to sequentially open the channels. Sample air was heated up to 180 °C to prevent condensation within the measurement chamber. On days when measurements changed between unit A and B (Fig. 1), the FTIR device was provided pure N_2 gas to zero its values. There was no need to correct data for deviations from zero.

An INNOVA gas monitor 1312 (Lumasense Technologies SA, Ballerup, Denmark; accuracy: ±1%) was connected to the flux chamber to determine gas production rates.

Measurement values from both devices were corrected based on lab calibrations and converted from ppm to $g\ m^{-3}$ with Eq. (3).

$$C_{x,i} = \frac{C_{x,i}[ppm]}{1 \cdot 10^6} * \frac{M_x}{M_{air}} * \rho_{air} \left(g\ m^{-3}\right) \tag{3}$$

Here, $C_{x,i}$ is the gas concentration of gas *x* in alley *i*, either in ppm or $g\ m^{-3}$; M_x the molar mass of gas x; M_{air} the molar mass of air (28.96 $g\ mol^{-1}$); ρ_{air} the density of air ($1.22 \cdot 10^3\ g\ m^{-3}$ at an average temperature of 12.7 °C).

Slurry level was measured with a measuring stick through the slots of the slatted floor.

2.7. Ventilation rate

After rewriting Eq. (1), Eq. (4) was used to quantify the ventilation rate of alley *i* for a certain moment in time.

$$VR_i = \frac{V_{hs,i} * dC_{x,i} - PR_x * A_i * SL * dt}{\left(C_{x,in} - C_{x,i,out}\right) * dt} \left(m^3\ h^{-1}\right) \tag{4}$$

with V_i the headspace volume of alley *i* (alley 1 to 5), PR_x production rate of gas x (CO_2 or CH_4). $dC_{x,i}$ the concentration difference in $g\ h^{-1}$ between *t* and *t*-1 in alley *i*. A_i is the slurry area of alley *i*. $C_{x,in}$ is the concentration of house air and $C_{x,i,out}$ is the headspace concentration averaged per alley per measurement cycle which had a time interval of 2 h.

2.8. Rate-of-decay

The ROD experiment was executed in alley 1 of unit A after the measurement period ended. A fair comparison between ventilation rate estimation by the ROD approach and the mass balance approach was still assumed since none or little effect of wind on pit ventilation rates was expected due to the closed curtains and mechanical ventilation in both units. Pure CO_2 gas was used as a tracer. CO_2 gas was injected via 9 injection points (Fig. 2B) in the middle of the headspace at a rate of $4.8\ l\ min^{-1}$. Orifices (flowrate 484 ± 51 ml min^{-1} at a pressure of 200 kPa) were used to assure homogeneous injection along the 9 injection points. To prevent direct measurement of the injected gas, injection points were placed at a maximum distance to the measurement points. During injection, headspace concentrations at locations 1 to 6 were measured with the FTIR analyser. Injection was stopped when 5000 ppm CO_2 was observed at one of the sampling locations. Measuring one sampling point took 90 s of which 30 s was flushing and three times 20 s for measuring.

During the ROD experiment, headspace height was 0.85 m and management was as usual (all doors and curtains were closed and cows were present in the unit). Although CO_2 has a higher molar weight compared to air (44.01 vs 28.96 g mol^{-1}), good mixing with headspace air was assumed since CO_2 was injected at a pressure of 200 kPa such that some turbulence near the injection point is created stimulating the mixing with air.

Concentration decay of CO_2 was described by Eq. (5) (Mosquera, 2002).

$$C_{x,i}(t) = C_{x,in} + \left(C_{x,i,0,hs} - C_{x,in}\right) * exp^{-\frac{\frac{VR_i}{3600} * t}{V_{hs,i}}} \left(g\ m^{-3}\right) \tag{5}$$

With gas $x = CO_2$ and alley $i = 1$. $C_x(t)$ is the CO_2 concentration in alley 1 of unit A at time t (s), $C_{x,in}$, the inflowing concentration, $C_{x,i,0,hs}$ the headspace concentration at t = 0, VR_i the ventilation rate through the headspace ($m^3\ h^{-1}$) and V_i the headspace volume which was 34.9 m^3. From the data of two repetitions, the model was fitted via a non-linear model regression in which $C_{x,in}$, $C_{x,i,0,hs}$ and VR_i were estimated. This analysis was performed with Genstat 19.

2.9. Statistical analysis of headspace gas concentrations

Data was analysed with R software for statistical computing (version 4.0). A datapoint was defined as the mean value of all concentration measurements per alley (or house air) during one measurement cycle, resulting in one datapoint every 2 h. Before analysis, normality of the data was checked with the Shapiro–Wilk test.

Variation in the datapoints over time was quantified by the coefficient of variation (CV). Observed variation was split in variation between days and within days. Between-days variation was computed with Eq. (6).

$$CV_{x,i} = \frac{SD_{x,i}[ppm]}{C_{x,i}[ppm]}(-) \tag{6}$$

Where standard deviation $SD_{x,i}$ and average $C_{x,i}$ are based on the average daily concentrations of gas x (CO_2 or CH_4) in ppm per alley i (i = alley 1–5 and house air). Within-day coefficient of variation per alley i and was computed in two steps. The CV per day j (j = day 1–21) was computed with Eq. (7) and summarised for the total measurement period with Eq. (8).

$$CV_{x,i,j} = \frac{SD_{x,i,j}[ppm]}{C_{x,i,j}[ppm]}(-) \tag{7}$$

$$CV_{x,i} = \sqrt{\frac{\sum_{j=1}^{n}\left(CV_{x,i,j}\right)^2}{n}}(-) \tag{8}$$

2.10. Statistical analysis of ventilation rates

Each measurement cycle of 2 h resulted in one ventilation rate estimation per alley i. A ventilation rate datapoint was defined as a single estimation per alley. Positive ventilation rates were selected since negative ventilation rates are not meaningful and from this data, outliers were removed per alley. The criterium for removal is provided in Eq. (9); Q_1, Q_3 are the first and third quartile and IQR is the interquartile range. Because of this criterium, between 7% (13 of 187) and 11.5% (24 of 209) of the datapoints per alley were excluded.

$$Q_1 - 1.5 * IQR < x < Q_3 + 1.5 * IQR \tag{9}$$

Ventilation rate estimations between alleys were compared based on the non-parametric Kruskal–Wallis test in combination with the Mann–Whitney U test.

A linear regression model with a Gaussian error distribution was set up to study the explanatory value of indoor temperature and slurry level on ventilation rates. R^2_{adj} was used as measure to explain observed variation. Eq. (10) shows the regression model.

$$y = \beta_1 * T + \beta_2 * SL + \varepsilon \tag{10}$$

3. Results and discussion

3.1. Headspace concentrations

Different concentration levels were observed between the pits as well as between the alleys as presented in Table 1. CO_2 concentration levels of 653–1082 ppm and 2639–6807 ppm were found beneath the slatted and closed floor respectively. CH_4 concentration levels were 29–98 ppm (slatted floor) and 320–930 ppm (closed floor). The headspace CO_2 and CH_4 concentration for the slatted floor had a right-skewed distribution, whereas headspace concentrations beneath the closed floor were left-skewed. For none of the individual alleys a normal distribution could be assumed. No significant difference in house air between both units was found, confirming our assumption of unit equality.

Variation between alleys was found for both the slatted and the closed floor. Regarding unit A, higher CO_2 and CH_4 concentrations were measured in alley 3 and 5 located beneath the cubicles compared to alleys 1, 2 and 4 which are covered with the slatted floor. Assuming a similar slurry gas production throughout the slurry pit, lower air exchange rates are present in the alleys located beneath the cubicles. In alley 1 of unit A, the average CO_2 concentration in alley 1 (653 ppm) was below the concentration of house air (664 ppm). Therefore, the assumption that house air composition represented the air flowing into the pit might not be valid.

Table 1 – Mean CO_2 and CH_4 concentration and standard deviation (per sampling point between measurements in time), the median and coefficient of variation (CV) for house air and per alley for both units during the measurement period. Alleys covered by slats in unit A are shaded grey. The rows 'total' summarise the coefficients of variation for alley 1–5 for the individual units.

		CO_2		CV-CO_2		CH_4		CV-CH_4	
		Mean ± SD (ppm)	Median (ppm)	Between days (–)	Within day (–)	Mean ± SD (ppm)	Median (ppm)	Between days (–)	Within day (–)
Unit A Slatted floor	House air	664 ± 109	686	0.08	0.16	27 ± 10	28	0.16	0.37
	Alley 1	653 ± 134	640	0.12	0.15	29 ± 21	25	0.42	0.44
	Alley 2	775 ± 258	717	0.22	0.20	44 ± 35	33	0.50	0.43
	Alley 3	861 ± 320	769	0.26	0.21	61 ± 52	45	0.56	0.42
	Alley 4	731 ± 174	708	0.15	0.16	36 ± 23	31	0.40	0.40
	Alley 5	1082 ± 334	986	0.23	0.20	98 ± 59	78	0.46	0.38
	Total A			**0.20**	**0.19**			**0.47**	**0.41**
Unit B Closed floor	House air	681 ± 90	680	0.09	0.12	26 ± 8	27	0.20	0.28
	Alley 1	2639 ± 923	2455	0.35	0.11	320 ± 155	292	0.50	0.16
	Alley 2	3442 ± 1367	3761	0.41	0.08	359 ± 152	395	0.44	0.11
	Alley 3	3151 ± 1241	3368	0.41	0.08	351 ± 149	396	0.44	0.09
	Alley 4	6629 ± 3605	8692	0.55	0.09	930 ± 544	1275	0.59	0.12
	Alley 5	6807 ± 3771	9003	0.56	0.08	919 ± 529	1246	0.58	0.11
	Total B			**0.46**	**0.09**			**0.51**	**0.12**

Spatial variation in CO_2 and CH_4 concentrations was also found in unit B where the closed floor was installed. Concentration levels were multiple times higher compared to unit A. The concentration levels in alley 4 and 5 which are significantly higher compared to alleys 1, 2 and 3 are remarkable. Either the slurry gas production rate is higher in alley 4 and 5 or the ventilation rate through alley 1, 2 and 3 is higher. The latter explanation is most plausible, but could not be underpinned with other data. In alley 1 and 4 of unit B a disposal valve for the manure scraper was present, but lowest concentrations were found in alley 1, 2 and 3. In both units, highest concentrations for both CO_2 and CH_4 were measured in alley 5. As presented in Fig. 2, this alley was covered with cubicles and had a dead end where air movement was expected to be smallest.

Variation within day and between days is presented in Table 1 and shows differences between both floors. According to our expectations, variation within a day was smaller for the closed floor than for the slatted floor. Variation between days was higher for the closed floor since the period of concentration accumulation was included in the dataset where average concentration levels increased from 992 to 6226 ppm for CO_2 and from 77 to 818 ppm for CH_4.

3.2. *Explanation of variation in headspace concentrations*

Variation in headspace concentrations was explained with the explanatory variables: indoor temperature, slurry level (only for between days) and diurnal pattern (only for within days). Daily temperature was correlated to slurry level as both increased over time during the measurement period. However, no physical relationship is present between these variables. Because of the correlation, R^2_{adj} of both the individual variables and the combined model was given in Table 2. Slurry level had a higher explanatory value for the closed floor (unit B) compared to the slatted floor (unit A). Slurry level explained a substantial part of the between-day variation except for alley 1. During the measurement period, slurry level increased with 8.3 mm per day. As a result, the absolute gas production increased due to a larger slurry volume while at the same time the headspace volume decreased. Consequently, headspace concentrations increased over time.

Indoor temperature explained a large part of the variation in pit concentrations between days of unit A (52%–86%). A second order linear model explained the effect of temperature on headspace concentrations best which is shown in Fig. 3. The second order relation – within this temperature range – can be physically explained by the thermal buoyancy effect. Headspace air is expected to have a constant temperature as a result of the slurry volume buffering temperature. At indoor temperature below headspace temperature, the cold air replaces headspace air as a result of a density difference. This led to an increase in pit ventilation as well as an increased removal rate of CO_2 and CH_4 produced by the slurry. Figure 3 shows increased concentrations above 8–10 °C indoor, suggesting that air exchange decreased with increasing indoor temperature. A similar pattern was found by Monteny (2000) who also measured headspace temperature. He found increased ventilation rates at indoor temperatures below headspace temperature.

A strong correlation ($R^2 = 0.99$) was present between CO_2 and CH_4 concentrations. Therefore, explained variation by the different models as presented in Table 2 was for both CO_2 and CH_4 in the same range. A difference in explained variation for all models in unit A is present between alley 1–4 and alley 5. The difference in alley 5 compared to alleys 1–4 is the full coverage by cubicles and a dead end which is expected to reduce air exchange and lead to different variation patterns. Slurry level had a higher explanatory value for alley 5 (55–71%) compared to alley 1–4 (23–38%). Next to that, indoor temperature explained more variation in alley 1–4.

Table 2 – Explained variation (R^2_{adj}) of between-day and within-day variation. The combined model existed of both explanatory variables. A second order polynomial model was used to describe the temperature effect. (–: not significant).

		Between days						Within day					
		R^2_{adj} indoor temperature (%)		R^2_{adj} slurry level (%)		R^2_{adj} combined model (%)		R^2_{adj} indoor temperature (%)		R^2_{adj} slurry level (%)		R^2_{adj} combined model (%)	
		CO_2	CH_4	CO_2	CH_4	CO_2	CH_4	CO_2	CH_4	CO_2	CH_4	CO_2	CH_4
Unit A Slatted floor	House air	27	48	–	17	26	48	–	–	38	41	38	41
	Alley 1	75	77	27	31	76	80	17	27	44	51	53	57
	Alley 2	82	80	28	23	85	80	21	22	26	33	36	40
	Alley 3	86	85	27	27	88	87	22	28	34	41	40	44
	Alley 4	84	89	37	38	92	96	30	32	14	21	38	39
	Alley 5	52	43	55	71	73	82	4	7	7	–	12	11
Unit B Closed floor	House air	–	–	–	–	–	–	–	7	9	25	9	26
	Alley 1	–	–	25	31	38	42	4	4	–	–	–	–
	Alley 2	–	–	60	62	60	63	–	–	–	–	–	–
	Alley 3	–	–	51	56	53	59	–	–	7	7	–	6
	Alley 4	–	–	87	84	86	87	–	–	13	–	13	–
	Alley 5	–	–	88	83	87	87	–	–	17	15	16	15

Within-day variation could only partly be explained by the explanatory variables. The diurnal pattern was described by assigning each hour of the day as a separate explanatory variable. The diurnal pattern explained most variation in house air and the alleys 1 and 3. The diurnal pattern was characterised by concentration drops for both CO_2 and CH_4 around 06:00. and 16:00 when the cows were milked. As shown in Fig. 4, these concentration drops were also found in alley 1 in both the morning and afternoon while in alleys 2–5, only a concentration drop in the morning was present. This suggests that alley 1 has a higher ventilation rate compared to alleys 2–5 and that the ventilation rate during night is higher compared to the ventilation rate during daytime. The explained variation by the diurnal pattern beneath the closed floor is small and expected to not be physically meaningful.

3.3. *Gas production rates*

The linear regression to obtain a_x resulted in regression coefficients of 0.98 (95% CI [0.97; 0.98]) for CO_2 and 0.90 (95% CI [0.87; 0.93]) for CH_4. CO_2 production per unit of slurry volume was found to be constant throughout the measurement period at 0.55 g [CO_2–C] m^{-3}_{slurry} h^{-1}, while the CH_4 production per unit of slurry volume increased from 0.09 g [CO_2–C] m^{-3}_{slurry} h^{-1} to 0.29 g [CO_2–C] m^{-3}_{slurry} h^{-1} within the 36 days of the measurement period. As a result, the CH_4–C/CO_2–C ratio changed. Sommer, Petersen, Sørensen, Poulsen, and Møller (2007) found the CH_4–C/CO_2–C ratio of the slurry gas production to be related to slurry temperature and the amount of inoculum. At low temperatures, they found CO_2 to be the main decomposition product, whereas CO_2 and CH_4 were produced

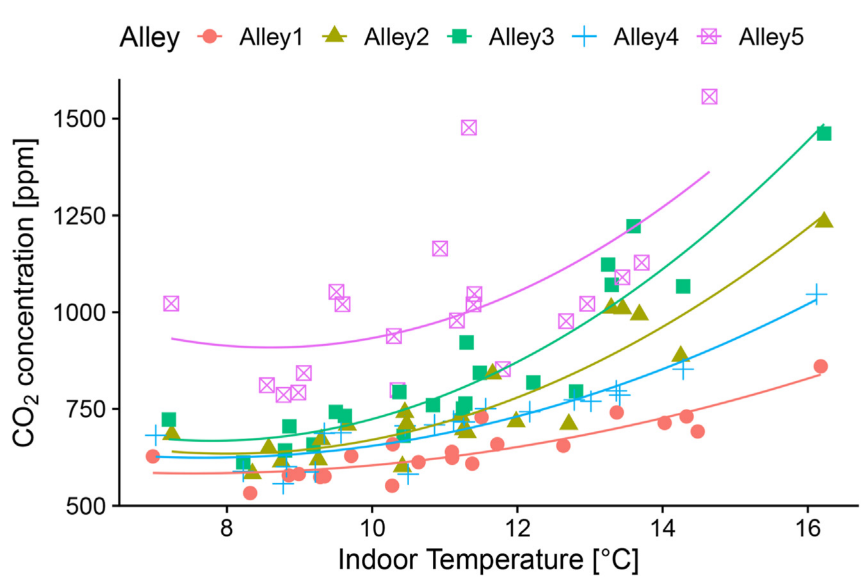

Fig. 3 – Average daily CO_2 concentration in the headspace of the five alleys versus average indoor temperature of unit A which was equipped with a slatted floor. Data points and second order polynomial regression lines per alley.

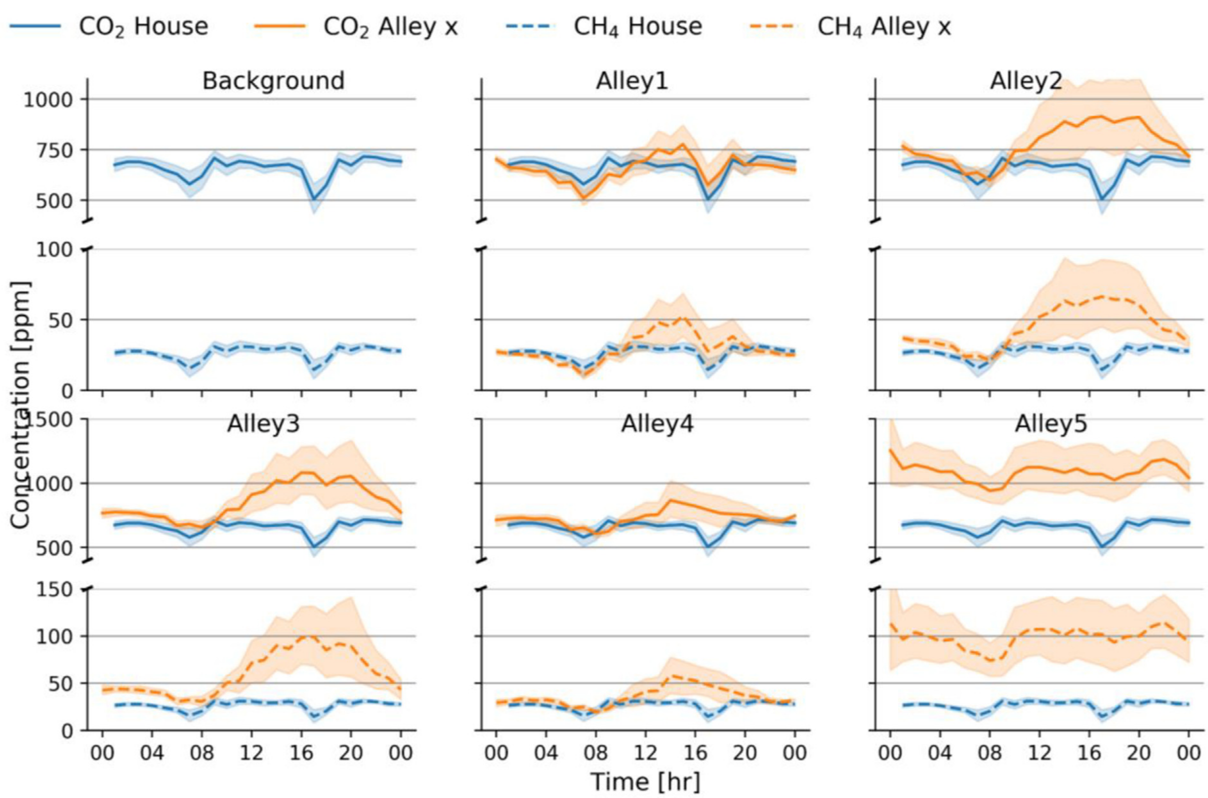

Fig. 4 – Diurnal patterns of the CO_2 and CH_4 concentration (± standard deviation between days) in the house air of unit A (called 'Background') and in the headspace air of the five alleys of the slurry pit. Background patterns are shown together with the pattern of each specific alley.

in equal amounts (on carbon-base) at a slurry temperature of 20 °C. Following that, the initial CH_4 production rate was determined by the amount of inoculum (pool of methanogens) (Sommer et al., 2007). In our study, the pits were cleaned in advance, and thus no inoculum was present. The period to reach maximum CH_4 production rate can take up to 200 days (Zeeman, 1991) meaning that in this study maximum CH_4 production rates were not reached. The spatial variation in gas production rate within unit A was up to 122% (relative to the mean production rate per day) for CO_2 and up to 250% for CH_4. More research is needed to investigate the cause of such variations.

3.4. *Rate-of-decay experiment*

The ROD experiment resulted in decay curves as shown in Fig. 5A. Figure 5B shows spatial variation throughout the alley, showing that headspace air is not perfectly mixed. At the start of the decay period, CO_2 concentration was highest (5616 ppm) at sampling point 2 and lowest (635 ppm) at sampling point 6. This observation is in accordance with the results of Qin et al. (2020) showing that fresh air enters the pit at the downwind side (sampling location 6) and recirculates to the upwind side (sampling location 1) causing spatial differences within the pit alley.

The non-linear regression model is plotted in Fig. 5A as 'predicted' and resulted in parameter estimates (± standard error) for C_{in} and C_0 of respectively 578 ± 122 ppm and 1993 ± 89 ppm. The estimation of the CO_2 concentration of the air flowing into the pit (C_{in}) was lower compared to the CO_2 concentration inside unit A (664 ± 8 ppm). Therefore, the assumption of house air representing inflowing air was expected to be invalid. This gave rise to the hypothesis that air flowing into the pit is a mixture of both house and outside air. Based on a CO_2 concentration of 412 ppm in the outside air (Friedlingstein, Jones, O'Sullivan, Andrew, & Bakker, 2022), 664 ppm in the house air (Table 1) and 578 in the air flowing into the pit, the fraction of outside air entering the slurry pit is 34%.

Based on the ROD, a ventilation rate of 173 ± 46 $m^3\ h^{-1}$ was calculated. With a headspace volume of 29.6 m^3, the headspace air replacement rate was between 4.3 and 7.3 h^{-1}.

3.5. *Headspace ventilation rates*

Ventilation rate estimations resulting from the mass-balance method are presented in Table 3. Different results were found based on the CO_2- and CH_4-based mass balances. Mean headspace ventilation rates in unit A were 149 $m^3\ h^{-1}$ and 353 $m^3\ h^{-1}$ for CO_2 and CH_4 respectively. In unit B, headspace ventilation rates were estimated to be 7 $m^3\ h^{-1}$ and 17 $m^3\ h^{-1}$ for CO_2 and CH_4 respectively. The CO_2 based ventilation rate of 286 $m^3\ h^{-1}$ in alley 1 of unit A was closer to the ROD based estimation of 173 $m^3\ h^{-1}$ compared to CH_4 (837 $m^3\ h^{-1}$).

The ROD experiments were not carried out on the same day as the mass-balance evaluations. This could explain part

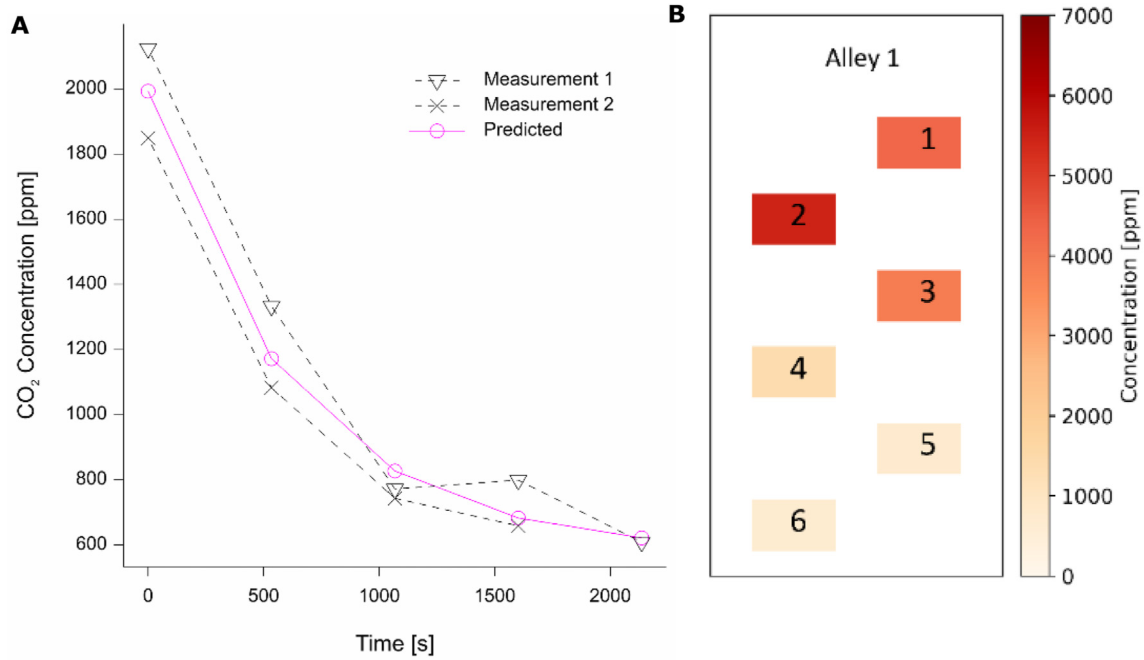

Fig. 5 – Left: decay curves from the ROD experiment in alley 1 of unit A. Measurement points are averaged values per measurement cycle of 540 s. Right: the spatial distribution within alley 1 by showing the CO_2 concentration per location at t = 0.

of the difference between the ventilation rate based on the ROD and based on the CO_2- and CH_4 mass balances. Nevertheless, the true ventilation rate is expected to be closest to the ROD based estimation since the ROD method has no need to know the concentration of the inflowing air which was most hard to estimate. Based on the decay-curves as discussed in the previous section, the real concentrations of the inflowing air are expected to be lower than the concentrations measured in the house air. If so, ventilation rates based on the CO_2- and CH_4 mass balances will decrease.

The ventilation rate based on the mass balance of CO_2 and CH_4 should be similar since measurements were taken simultaneously. Therefore, the sources of error could be: (1) a misestimation of the inflowing air concentration, (2) a measurement error in headspace concentration measurements or (3) a measurement error in gas production rate. If the air flowing into the pit has a different CH_4–CO_2 ratio compared to the house air, different effects will be visible in ventilation rates for CO_2 and CH_4. A larger measurement error can be expected for methane if also volatile organic compounds (VOC) are present, but not taken into account in the FTIR measurement device (Kohl et al., 2019). Indeed, no interference effect with VOC's was accounted for by our measurement instrument. Since for CO_2 all interferent gasses were

Table 3 – Ventilation rate (VR) estimations (± standard error) based on the mass balances of CO_2 and CH_4 split up between day (6:00–21:59) and night (22:00–5:59). N = 8–133 per alley per day period.

		VR based on mass balance CO_2		VR based on mass balance CH_4	
		Mean ± standard error [$m^3\ h^{-1}$]		Mean ± standard error [$m^3\ h^{-1}$]	
		Day	Night	Day	Night
Unit A (Slatted)	Alley 1	286 ± 42	790 ± 127	837 ± 144	2479 ± 455
	Alley 2	147 ± 14	283 ± 23	365 ± 35	573 ± 46
	Alley 3	93 ± 8	185 ± 12	158 ± 11	268 ± 15
	Alley 4	171 ± 19	240 ± 25	424 ± 46	574 ± 39
	Alley 5	48 ± 3	52 ± 4	88 ± 5	95 ± 6
	Mean	**149 ± 7**		**353 ± 7**	
Unit B (Closed)	Alley 1	13 ± 1	13 ± 1	32 ± 1	32 ± 2
	Alley 2	6 ± 0	6 ± 0	18 ± 0	17 ± 1
	Alley 3	7 ± 0	7 ± 0	18 ± 0	17 ± 1
	Alley 4	3 ± 0	3 ± 0	6 ± 0	7 ± 0
	Alley 5	4 ± 0	4 ± 0	8 ± 0	8 ± 0
	Mean	**7 ± 7**		**17 ± 7**	

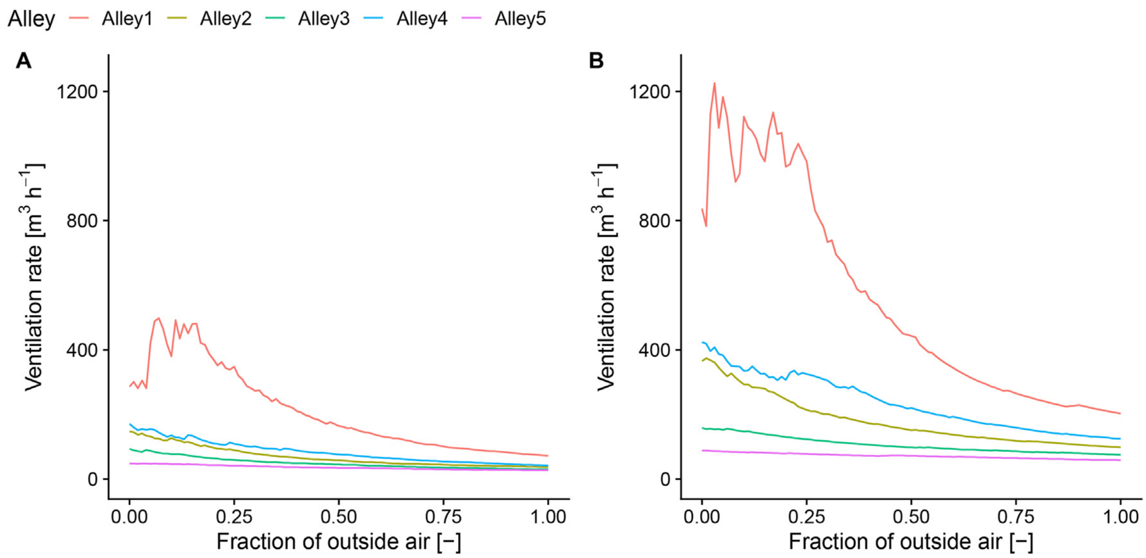

Fig. 6 – Calculated ventilation rates (Eq. (4)) for different mixing ratios between house and outside air in the air (expressed as fraction of outside air) flowing into the slurry pit. A gives the result based on the carbon dioxide mass balance and B the result for the methane mass balance. Note the difference in y-axis range.

measured, the CO_2 headspace concentrations are more accurate. Interference of VOC's also lead to inaccurate results with the photo-acoustic principle which was used to quantify the gas production rate (Liu et al., 2020). For follow-up research, it is recommended gas production rate is estimated using the same instrument as used for the headspace concentration measurements.

Nevertheless, variation patterns in headspace ventilation rate were consistent between CO_2 and CH_4. Both methods showed a difference in ventilation rate between day (6:00–21:59) and night (22:00–5:59) as well as between unit A and unit B. Variation between day and night is expected to be temperature driven. Temperature dropped during the night and pit ventilation rate increased up to three times as a result of cold air replacing headspace air according to the thermal buoyancy principle. This observation is confirmed by Fig. 4 showing increased headspace concentration levels compared to house air during daytime, but only small differences during night.

The difference in headspace ventilation between unit A and B can be designated to the floor type. Compared to the slatted floor, pit air exchange is reduced by 95% with a closed floor.

Significant differences in ventilation rate estimations were present between the alleys in unit A, except for alley 2 and alley 4. Alley configuration is expected to have an effect on ventilation rate since higher concentrations and thus lower ventilation rates were found in alley 3 and alley 5. These alleys were covered by cubicles which act as a closed floor. Besides this difference, the alleys also varied in surface area leading to smaller differences when the ventilation rate is expressed per square meter slurry surface per hour (VR in unit A for alley 1–5 respectively in $m^3\ m^{-2}{}_{slurry\ surface}\ h^{-1}$: 8.2, 6.1, 3.9, 7.1, 1.6).

As discussed on basis of the ROD results, the assumption that the gaseous composition of air flowing into the pit can be approached by house air is expected not to be valid. To study the effect of this assumption on the ventilation rates from the mass balance approach, a sensitivity analysis was performed. The fraction of outside air (CO_2: 400 ppm; CH_4: 1.8 ppm) in the inflowing air was varied in a range of 0–80%, based on the ROD estimation of inflowing air CO_2 concentration (578 ± 122 ppm). The effect of this varied mixing ratio on headspace ventilation rate is plotted in Fig. 6. An increased proportion of outside air in the inflowing air increases the concentration gradient between inflowing and headspace air and thus lowers the modelled ventilation rates. However, maximum ventilation rates were observed in alley 1 between 5 and 28% outside air. This is due to the fact that negative concentration gradients were excluded, but become positive at lower gas concentrations in the inflowing air.

The ventilation rate of 173 $m^3\ h^{-1}$ as estimated by the ROD experiment, was obtained with the CO_2 mass balance at a fraction of outside air of 0.5. Based on the CH_4 mass balance, ventilation rates are 250 $m^3\ h^{-1}$ at an outside air fraction of 0.8.

4. Conclusions

The temperature of the air flowing in the cow house determines pit ventilation rate. When the temperature of the outside air drops below the headspace air temperature, pit ventilation increases. As a result, a clear difference in ventilation rate between day and night was found in this study with ventilation rates during the night being up to three times higher compared to during daytime. Next to that, ventilation rate is significantly lower in alleys covered by cubicles compared to a slatted floor. A closed floor reduces air exchange between pit and house by 95% compared to a slatted floor.

Using the CO_2 and CH_4 mass balance of the slurry pit is most applicable to study relative effects in pit ventilation rate, since it is hard to estimate CO_2 and CH_4 concentrations of the air flowing into the pit accurately. For a more accurate quantification of the pit ventilation rate, a rate-of-decay experiment is applicable if enough sampling points are available to cover spatial differences.

Declaration of competing interest

The authors declare that they have no known competing financial interests or personal relationships that could have appeared to influence the work reported in this paper.

REFERENCES

Aguirre-Villegas, H. A., Wattiaux, M. A., Larson, R. A., Chase, L., Ranathunga, S. D., & Ruark, M. D. (2017). Dairy cow nitrogen efficiency. https://www.virtualfarm.psu.edu/assets/uploads/content/DairyCap_DairyCowNitrogenEfficiency-Final-Final.pdf. (Accessed 9 November 2018).

Amon, B., Kryvoruchko, V., Amon, T., & Zechmeister-Boltenstern, S. (2006). Methane, nitrous oxide and ammonia emissions during storage and after application of dairy cattle slurry and influence of slurry treatment. *Agriculture, Ecosystems & Environment, 112*(2), 153–162. https://doi.org/10.1016/j.agee.2005.08.030

Bleeker, A., Sluis, S.v. d., & Schijndel, M.v. (2018). Ammoniakemissie van de landbouw blijft gelijk. Retrieved from http://themasites.pbl.nl/balansvandeleefomgeving/jaargang-2018/themas/landbouw-en-voedsel/mest-en-ammoniak. (Accessed 18 September 2018).

Buswell, A., & Mueller, H. (1952). Mechanism of methane fermentation. *Industrial & Engineering Chemistry, 44*(3), 550–552. https://doi.org/10.1021/ie50507a033

CCAC. (2017). Climate and clean air coalition annual report. Retrieved from https://www.ccacoalition.org/en/resources/climate-and-clean-air-coalition-annual-report-2016-2017.

Chadwick, D., Sommer, S. G., Thorman, R., Fangueiro, D., Cardenas, L., Amon, B., et al. (2011). Manure management: Implications for greenhouse gas emissions. *Animal Feed Science and Technology, 166–167*, 514–531. https://doi.org/10.1016/j.anifeedsci.2011.04.036

EEA. (2016). *National emission ceilings (NEC) directive 2016/2284/EU*.

European Commission. (2020). *Stepping up Europe's 2030 climate ambition Investing in a climate-neutral future for the benefit of our people*.

Friedlingstein, P., Jones, M. W., O'Sullivan, M., Andrew, R. M., & Bakker, D. C. (2022). Global carbon budget 2021. *Earth System Science Data, 14*(4), 1917–2005. https://doi.org/10.5194/essd-14-1917-2022

FAO and GDP. (2018). *Climate change and the global dairy cattle sector - the role of the dairy sector in a low-carbon future* (p. 36).

Gerber, P., Vellinga, T., Opio, C., Henderson, B., & Steinfeld, H. (2010). *Greenhouse gas emissions from the dairy sector. A life cycle assessment*. Rome, Italy: Food and Agricultural Organization of the United Nations: Animal Production and Health Division.

Heij, G. J., & Schneider, T. (1991). *Acidification research in the Netherlands : Final report of the Dutch priority programme on acidification*. Amsterdam: Elsevier.

Hindrichsen, I. K., Wettstein, H. R., Machmüller, A., & Kreuzer, M. (2006). Methane emission, nutrient degradation and nitrogen turnover in dairy cows and their slurry at different milk production scenarios with and without concentrate supplementation. *Agriculture, Ecosystems & Environment, 113*(1), 150–161. https://doi.org/10.1016/j.agee.2005.09.004

Hoogerbrugge, R., Geilenkirchen, G., den Hollander, H., van der Swaluw, E., Visser, S., de Vries, W., et al. (2019). *Grootschalige concentratie-en depositiekaarten nederland: Rapportage 2019*.

Huis in 't Veld, J. W. H., & Monteny, G. J. (2003). Methane emission from cubicle housing systems for dairy cows. Retrieved from Wageningen: http://edepot.wur.nl/160043.

Knapp, J. R., Laur, G. L., Vadas, P. A., Weiss, W. P., & Tricarico, J. M. (2014). Invited review: Enteric methane in dairy cattle production: Quantifying the opportunities and impact of reducing emissions. *Journal of Dairy Science, 97*(6), 3231–3261. https://doi.org/10.3168/jds.2013-7234

Kohl, L., Koskinen, M., Rissanen, K., Haikarainen, I., Polvinen, T., Hellén, H., et al. (2019). Technical note: Interferences of volatile organic compounds (VOCs) on methane concentration measurements. *Biogeosciences, 16*(17), 3319–3332. https://doi.org/10.5194/bg-16-3319-2019

Liu, D., Rong, L., Kamp, J., Kong, X., Adamsen, A. P. S., Chowdhury, A., et al. (2020). Photoacoustic measurement with infrared band-pass filters significantly overestimates NH3 emissions from cattle houses due to volatile organic compound (VOC) interferences. *Atmospheric Measurement Techniques, 13*(1), 259–272. https://doi.org/10.5194/amt-13-259-2020

Monteny, G. J. (2000). Modelling of ammonia emissions from dairy cow houses. S.l. Retrieved from https://edepot.wur.nl/194569.

Monteny, G. J., Bot, G. P. A., Raaben, J. H. W., & Overbeek, J. P. E. (2000). Air exchange through a slatted floor for dairy-cow housing. Retrieved from https://edepot.wur.nl/194569#page=83.

Monteny, G. J., Schulte, D. D., Elzing, A., & Lamaker, E. J. J. (1998). A conceptual mechanistic model for the ammonia emissions from free stall cubicle dairy cow houses. *Transactions of the ASAE, 41*(1), 193–201. https://doi.org/10.13031/2013.17151

Mosquera, J. (2002). Meetmethoden gasvormige emissies uit de veehouderij (9054062169 9789054062165). Retrieved from Wageningen: https://edepot.wur.nl/384489.

Mosquera, J., Aarnink, A. J. A., Ellen, H. H., Van Dooren, H. J. C., Van Emous, R. A., Van Harn, J., et al. (2017). Overzicht van maatregelen om de ammoniakemissie uit de veehouderij te beperken : Geactualiseerde versie 2017. https://edepot.wur.nl/427311.

Moss, A. R., Jouany, J., & Newbold, J. (2000). Methane production by ruminants: Its contribution to global warming. *Annales de Zootechnie, 49*(3), 231–253. https://doi.org/10.1051/animres:2000119

Ogink, N. W. M., Groenestein, C. M., & Mosquera, J. (2014). Update of ammonia emission factors for cattle categories: Advisory report for amendments in regulations on ammonia and livestock. Retrieved from http://edepot.wur.nl/294436.

Ogink, N. W. M., Mosquera, J., Calvet, S., & Zhang, G. (2013). Methods for measuring gas emissions from naturally ventilated livestock buildings: Developments over the last decade and perspectives for improvement. *Biosystems Engineering, 116*(3), 297–308. https://doi.org/10.1016/j.biosystemseng.2012.10.005

Ogink, N. W. M., Mosquera, J., & Hol, J. M. G. (2017). Measurement protocol for ammonia emission from housing systems in livestock production 2013a. Retrieved from Wageningen: https://edepot.wur.nl/418425.

Qin, C., Wang, X., Zhang, G., Yi, Q., He, Y., & Wang, K. (2020). Effects of the slatted floor layout on flow pattern in a manure pit and ammonia emission from pit-A CFD study. *Computers and Electronics in Agriculture, 177*, Article 105677. https://doi.org/10.1016/j.compag.2020.105677

Šebek, L., & Schils, R. (2006). Verlaging van methaan-en lachgasemissie uit de Nederlandse melkveehouderij. Retrieved from https://edepot.wur.nl/27395.

Snoek, J. W., Stigter, J. D., Ogink, N. W. M., & Groot Koerkamp, P. W. G. (2014). Sensitivity analysis of mechanistic models for estimating ammonia emission from dairy cow urine puddles. *Biosystems Engineering, 121*, 12–24. https://doi.org/10.1016/j.biosystemseng.2014.02.003

Solomon, S., Qin, D., Manning, M., Marquit, M., Averyt, K., & Tignor, M. B. (2007). Climate change 2007: The physical science basis. Retrieved from https://www.ipcc.ch/site/assets/uploads/2018/05/ar4_wg1_full_report-1.pdf.

Sommer, S. G., Petersen, S. O., Sørensen, P., Poulsen, H. D., & Møller, H. B. (2007). Methane and carbon dioxide emissions and nitrogen turnover during liquid manure storage. *Nutrient Cycling in Agroecosystems, 78*(1), 27–36. https://doi.org/10.1007/s10705-006-9072-4

Starmans, D. A. J., Blanken, K., Kupers, G. C. C., & Timmerman, M. (2009). Schuimvorming op mest: Eindrapportage (1570-8616). Retrieved from https://edepot.wur.nl/14942.

Sutton, M. A., Erisman, J. W., & Oenema, O. (2007). Strategies for controlling nitrogen emissions from agriculture: Regulatory, voluntary and economic approaches paper presented at the fertilizer best management practices. Brussel https://mhchem.org/221/wq/Fertilize/FBMP.pdf#page=252.

TacRav. (2018). Hoofdcategorie A: Rundvee. Retrieved from https://www.infomil.nl/onderwerpen/landbouw/ammoniak/rav-0/bijlage-1/emissiefactoren-per/map-staltypen/hoofdcategorie/Last. (Accessed 27 September 2018).

Van Dooren, H. J. C., & Smits, M. C. J. (2007). Reductieopties voor ammoniak-en methaanemissie uit huisvesting voor melkvee= Reduction options of ammonia and methane emissions from dairy housing. https://edepot.wur.nl/22422.

Ye, Z., Zhang, G., Seo, I. H., Kai, P., Saha, C. K., Wang, C., et al. (2009). Airflow characteristics at the surface of manure in a storage pit affected by ventilation rate, floor slat opening, and headspace height. *Biosystems Engineering, 104*(1), 97–105. https://doi.org/10.1016/j.biosystemseng.2009.05.005

Zeeman, G. (1991). Mesophilic and psychrophilic digestion of liquid manure. Zeeman, S.l. Retrieved from http://edepot.wur.nl/202851.